Effect of Velocity Profile on Turbulent Flow and Mixing in T-Junction

Boumaza Mokadem, Amina Lyria Cheridi Deghal, Ahmed Dahia, Salah Medguedem

[1]Nucear Rsearch Centre of Birine, B.P 180 Ain Oussera 17200
Djelfa, Algeria
*Corresponding author; email: m.boumaza@crnb.dz

Article Info

Article history:

Received , 28/04/2024
Revised , 30/05/2024
Accepted , 12/06/2024

Keywords:

T-junction
Mixing
RANS
LES
Temperature fluctuations

ABSTRACT

The study contributes to a better understanding of the thermal mixing phenomena that occur at T-junctions and emphasizes the significance of the inlet velocity profile in affecting the dynamic and thermal characteristics of the flow. Ansys CFX version 19.1 was used to examine the dynamic and thermal behavior of turbulent flow in a T-junction, employing two turbulence models: URANS (SST) and LES with a power law velocity profile. The obtained results offer useful information for creating suitable geometric layouts and optimizing pipe systems. The study hypotheses were validated by comparing the obtained results with the experimental data from the Vattenfall facility. The velocity and temperature fields were calculated at multiple locations downstream of the junction. As will be shown in the results section, there was a good agreement between simulation predictions and experimental data.

I. Introduction

The turbulent thermal mixing phenomenon is a complex process that occurs in many industrial installations, such as chemical reactors, heat exchangers, cooling towers, boilers, etc. As a result of the fluids being mixed at various temperatures, there may be substantial mass and heat fluxes. The chaotic and random fluid movements that define turbulent and thermal mixing are brought on by shear and turbulence forces [01]. These motions produce eddies and vortices that encourage fluid mixing and expand their contact surfaces. Turbulent and thermal mixing can be employed in industrial settings to quickly cool heated fluids, speed up chemical reactions, regulate temperature, and more. Significant pressure losses, corrosion concerns, phase separation problems, etc. might also result from this process. Understanding the characteristics of the employed fluid, the operating circumstances, the fluid mixing properties, and the equipment geometry are crucial for optimizing turbulent thermal mixing in industrial systems [02].

The mixing phenomenon is the result of the injection of cold water into hot water due to industrial requirements through a T-junction brunch, which can create a mixing zone downstream of this mechanical system (Fig. 1). Poor mixing (heterogeneous mixing) between the hot and cold fluids can lead to thermo-physical problems such as cold shock, thermal fatigue that can cause cracks in the walls, and stratification [03]. The temperature distribution along the mixing zone varies over time, and the frequency of occurrence of mixing heterogeneity can influence the structural integrity of systems that requires a uniform temperature distribution [04].

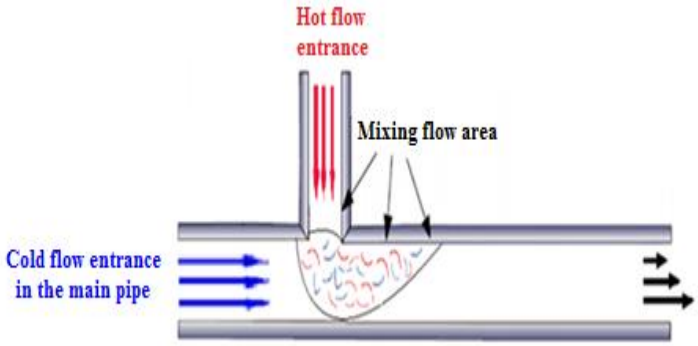

Figure 1. Schematic of turbulent flow in T-junction branch (reproduced by the authors) [03].

In the literature review section, we have provided a state-of-the-art overview of the thermal mixing phenomenon encountered in the industry. In most of the experiments and theory it is mentioned that the thermal mixing is the main cause of fatigue, which depends on temperature fluctuations near the pipe wall. An important experimental investigation was reported by Hirota et al., (2006) [05] on turbulent mixing of hot and cold airflow in a T-junction of an automotive air conditioning system. In this system, the branch flow was separated at the edge of the T-junction and forms a large separation bubble. As results, they observed the formation of a longitudinal vortices around the separation bubble, and the average temperature in the thermal mixing layer present a uniform spanwise distributions. Walker et al., (2009) [06] have established an experimental device of a T-junction with wire-mesh sensors at high resolution in time and space. The practical realization aims to measure and predict the transient flow field of a turbulent mixing downstream of the connection. They found the presence of several flow regions near the mixing zone, which differ in their temperature values and vorticity. In order to determine the performance of the supercharging system, Kun Zhang et al., (2021) [07] were developed a new T-junction model to study the transfer and energy conversion of exhaust gases flowing through the junctions of the exhaust manifold. Some tests on the influence of thermodynamic parameters, such as compressibility of gases and the pressure loss coefficient, on the flow in the T-junction has been effectively approved.

To see the reliability of Large Eddy Simulation turbulent model to describe the temperature fluctuations intensity in mixing T-junction, Wei-yu Zhu et al., (2009) [08] have simulate the normalized mean and root mean square temperatures and analyzed the effects of Reynolds number and Richardson number under different conditions. Simoneau et al., (2010) [09] have performed an interesting compilation of Large Eddy Simulations related to the nuclear domain to assess the thermal and pressure fluctuations quantities in Tee junctions by mean of flow over obstacles, and parallel shear flows. As results, they conclude that the LES model become a more standard tool in fluid engineering. Frédéric et al., (2012) [10] targeted the efficiency of thermal power plants using high levels of temperatures. The numerical approach used involves LES in the branch of T-junction pipe. They were able to prepare a maps of thermal fluctuations at a mixing Tee for nuclear power station application. They observe a significant temperature difference expected between the turbulent flows of the coolants which converge at the level of certain mixing Tees. As the thermal balance does not occur instantaneously, the temperature fluctuations can develop and induce cracking in the pipes by thermal fatigue. Raphaël Monod, (2012) [11] studied the temperature fluctuations near the walls and assess the risk of thermal fatigue in the mixing Tee of thermal power plants using the Large Eddy Simulation. For this reason, a sensitivity study was made to see the influence of a low-number turbulent flow of Prandtl number on the temperature profiles. They estimated the length of the three branches of Tee using different temperature limit conditions, suh as; isothermal, isoflux and with thermal resolution in the wall.

To provide a suitable validation of CFD-calculations and to predict thermal mixing in T-junction, some comparisons with different models (LES, DES, RANS, URANS) were made. Westin et al., (2009) [12] set up a new experimental data device for comparison purpose with LES and DES approaches. The data was obtained from temperature measurements with thermocouples located near the pipe wall. The simulation with LES gives a poor predictions of the mean velocity near the wall, while the simulations using DES improved the near-wall velocity predictions and failed to predict the temperature fluctuations. Similar conclusions were found by (Mi Zhou et al., 2022., Liu et al., 2013., Kimura et al., 2010) [13-15] using numerical simulations, which have been performed with different flow temperature using Large Eddy Simulation approach. The reported findings provide a good illustration of flow distributions in mixing behavior due a high temperature differences. Yacine et al., (2012) [16] predict by numerical simulation the thermal mixing in T-junction using Large Eddy Simulation (LES) and Shear Stress Transport model (SST) approaches in flow channel at Re=395. This work was compared and validated by

an experimental devise. Both codes give a satisfactory result in solving the problems related to the numerical dissipation. The LES approach proves its capability to reproduce correctly the flow behavior and even providing instantaneous data satisfactory for fatigue assessment under thermal stress, where URANS technique is capable to predicting the mean variables of the turbulence flow. Lu et al., (2015) [17] made a study analysis on thermal fluctuations caused by turbulent penetration and buoyancy effects in a T-pipe with a closed branch pipe by applying the turbulence model LES. To eliminate the thermal fluctuations, a vortex breaker has been integrated into the branch pipe. The numerical results show that with this modification, the risk of thermal fatigue caused by thermal fluctuations was effectively reduced.

All these studies are more frequently applied in nuclear reactors, where a various number of T-junctions can be found in the safety injection system. In case of accidental depressurization, a nonlinear distribution of the temperature in this system, including the turbulent injection of the cooling liquid can be found. The safety injection system is connected to supply the reactor cooling system by mixing a boric acid solution to remove excessive residual heat.

In the light of the previous state of art, we try to estimate the properties of the injection fluid and evaluate the mean flow field, the velocity and temperature of turbulent mixing flow in and around of a T-junction brunch. For this purpose, we use the CFD approach to study the dynamic and thermal behavior of the turbulent mixing of two flows (hot and cold) in a simple geometric configuration (T-junction) with different temperature and flow velocity to create a mixing zone downstream of the concerned configuration. Two turbulence models, URANS (SST) and LES (Large Eddy Simulation), are employed with a power law velocity profiles using Smagorinsky–Lilly at the inlet of each pipe. The obtained results must be compared with the available experimental data of Vattenfall facility [3].

II. Material & methods

II.1. Experimental study

In order to accurately assess the probability of the occurrence of unacceptable defects in all T-connections in the piping system and optimize technical maintenance cycles, it is necessary to study the characteristics of changes in the local flow structure (temperature, velocity, and pressure) and investigate the mechanisms responsible for any changes in the local properties of the introduced flow [18]. Originally, these tasks led experimenters to include measurement using well-known methods such as thermocouples, optical fibers, as well as laser Doppler velocimetry (LDV/PIV systems). The obtained values helped to gain a better understanding of the mixing phenomenon as a function of Reynolds number, taking into account variations in flow velocity at the boundary between the main flow and the incoming flow [19]. An experimental device of fluid dynamics with circular cross-sections and T-junctions was selected to evaluate the peculiarities of the influence of shear layer oscillations, formed in the area between the transverse flow and the incoming flow, on mixing efficiency [20].

In this work, for better understanding thermal mixing phenomena in T-junctions and to predict the velocity and temperature fluctuations during thermal mixing, a benchmark study including recent results with data obtained from the Vattenfall experimental test rig were exploited (Fig. 2). The experimental device was made by a horizontal pipe, which represent the main cold pipe with inner diameter (D2) of 140 mm, and a vertical pipe for hot water with inner diameter (D1) of 100 mm. The upstream length of the cold pipe is more than 80 pipe diameters from the origin of the axis to the outlet, and the total distance upstream of the T-junction is approximately 20 pipe diameters (Fig. 2).

A constant flowrate by a rotate pump was used to supply the device with high level reservoir of 80 m3. Two stagnation chamber; one is mounted in the cold-water leg (diameter 400 mm), the side where the incoming water supply come via a flow distributor, and a second one is mounted in the hot leg (diameter 300 mm) giving an area contraction ratio of 9:1. The mean temperature, and temperature fluctuations were recorded at response time of 13ms using thermocouples mounted in the wall of the device at seven stations downstream of the T-junction.

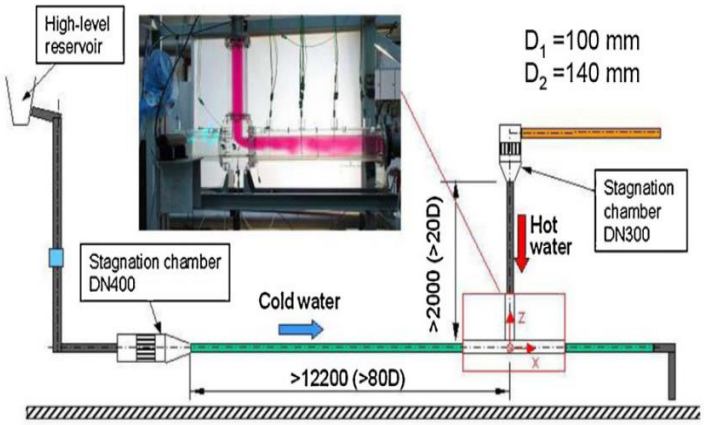

Figure 2. Side view of Vattenfall test rig [03, 21].

II.2. Numerical study

The simulation of turbulent flow and thermal mixing were performed by solving the Reynolds Averaged Navier Stokes (RANS) equations. In reality, it is rare for the velocity profile to be uniform in a pipe flow, for this a non-uniform and a fully developed turbulent flow at the inlet of each conduit carrying hot and cold fluid streams was considered.

The turbulence transport equation associated with a temperature scalar is an important mathematical expression for predicting and understanding the behavior of temperature fields in turbulent fluids. It is widely used in various fields of fluid mechanics, including combustion, heat transfer, and atmospheric sciences. This expression describes how the temperature scalar is transported by turbulent flows in a fluid. The equation takes into account the effects of turbulence, which can cause mixing, diffusion, and advection of the scalar. The general form of the convection-diffusion transport equation for a scalar quantity $\emptyset$ can be written [13-15]:

$$\underbrace{\frac{\partial}{\partial t}(\rho\phi)}_{1} + \underbrace{\frac{\partial}{\partial x_i}(\rho u_i \emptyset)}_{2} - \underbrace{\frac{\partial}{\partial x_i}\left(\Gamma_\phi \frac{\partial \emptyset}{\partial x_i}\right)}_{3} = \underbrace{S_\emptyset}_{4} \qquad (1)$$

Where $\emptyset$ represents the scalar quantity, ui the velocity vector, ρ the water density, μ the dynamic viscosity, Γ_ϕ the diffusion coefficient, and S represents any source terms.

The four terms numbered in the transport equation represent the processes by which the dependent variable $\emptyset$ is transported by the fluid:
1-Rate of change of the variable $\emptyset$,
2-Convection term,
3-Diffusion term,
4-Source term.

II.2.1 Governing equations with SST turbulence model

The selection of an appropriate turbulence model scheme is very crucial in the flow modeling. The *SST* (Shear Stress Transport) model was chosen in this work because it combines the robustness and the accuracy of k- ω model in the region close to the wall and the efficiency of k-ε far from the wall. The *SST* model is mainly advised for fluids may encounter unexpected stress changes. The link between the two formulations of the two models is made through a transient function which can be presented by the following equation [13, 22]:

$$SST = \alpha(k-\omega) + (1-\alpha)(k-\varepsilon) \qquad (2)$$

Where $\alpha = 0$ in the flow centerline and $\alpha = 1$ near the wall, k is the turbulent kinetic energy and ε is the dissipation

of the transport equations. The turbulent kinetic energy equation is given in Eq. (3) and the turbulent dissipation is expressed in Eq. (4), respectively [23, 24].

$$\frac{\partial}{\partial t}(\rho k)+\frac{\partial}{\partial x_i}(\rho k u_i)=\frac{\partial}{\partial x_j}\left[\left(\mu+\frac{\mu_t}{\sigma_k}\right)\frac{\partial k}{\partial x_j}\right]+P_k+P_b-\rho\varepsilon-Y_M+S_k \quad (3)$$

$$\frac{\partial}{\partial t}(\rho \varepsilon)+\frac{\partial}{\partial x_i}(\rho \varepsilon u_i)=\frac{\partial}{\partial x_j}\left[\left(\mu+\frac{\mu_t}{\sigma_\varepsilon}\right)\frac{\partial \varepsilon}{\partial x_j}\right]+C_{1\varepsilon}\frac{\varepsilon}{k}(P_k+C_{3\varepsilon}P_b)-C_{2\varepsilon}\rho\frac{\varepsilon^2}{k}+S_\varepsilon \quad (4)$$

Where the empirical coefficients are given as:

$$C_{1\varepsilon}=1.44,\quad C_{2\varepsilon}=1.92, C_\mu=0.09, \sigma_k=1.0\ and\ \sigma_\varepsilon=1.3$$

S is the main rate of strain tensor:

$$S=\sqrt{2S_{ij}S_{i,j}} \quad (5)$$

and $$P_k=-\rho\overline{u_i'u_j'}\frac{\partial u_j}{\partial x_i} \quad (6)$$

u_i is the velocity component in direction *i*, P_b define the effect of buoyancy, and P_{rt} is the turbulent Prandtl number for energy.

$$P_b=\beta g_i\frac{\mu_t}{Pr_t}\frac{\partial T}{\partial x_i} \quad (7)$$

β define the coefficient of thermal expansion given by: $\beta=-\frac{1}{\rho}\left(\frac{\partial \rho}{\partial T}\right)_P$ (8)

II.2.2 Governing equations with LES model

The Large Eddy Simulation (LES) equations described below, which include the mass conservation equation, the momentum conservation equation and the energy conservation equation, are obtained from Navier-Stokes equations. The LES model implemented in ANSYS-CFX platform is a three-dimensional and unsteady turbulence model. To separate the large from the small scales, LES solves Navier-Stokes equation by filtering the large-scale eddies and models the small-scale eddies through a subgrid-scale (SGS) model proposed by Smagorinsky [25-27]. This last is supposed provide an improved near-wall behavior, and increased transport and dissipation. The conservation of mass and momentum equations can be defined as [25]:

$$\begin{cases}\frac{\partial \rho}{\partial t}+\frac{\partial}{\partial x_i}(\rho\bar{u}_i)=0\\ \frac{\partial}{\partial t}(\rho\bar{u}_i)+\frac{\partial}{\partial x_j}(\rho\bar{u}_i\bar{u}_j)=\frac{\partial \sigma_{ij}}{\partial x_j}-\frac{\partial \bar{p}}{\partial x_i}-\frac{\partial \tau_{ij}}{\partial x_j}+\rho_0\beta(T-T_0)g_i\end{cases} \quad (9)$$

Where $\bar{u}$ and $\bar{p}$ are the velocity and pressure component. ρ_0 and T_0 are the reference density and temperature, g_i is the gravitational acceleration in ith direction.

$\partial\tau_{ij}$ represent the subgrid-scale stress, which is defined by,

$$\partial\tau_{ij}=\rho\overline{u_iu_j}-\rho\bar{u}_i\bar{u}_j \quad (10)$$

τ_{ij} can be expressed by: $\tau_{ij}-\frac{\tau_{kk}\delta_{ij}}{\varepsilon}=-2\mu_i\bar{S}_{ij}$

$\partial\sigma_{ij}$ is the stress tensor due to molecular viscosity (Eq. 11).

$$\partial\sigma_{ij}=\left[\mu\left(\frac{\partial\bar{u}_i}{\partial x_j}\right)+\frac{\partial\bar{u}_j}{\partial x_i}\right]-\frac{2}{3}\mu\frac{\partial\bar{u}_i}{\partial x_i}\delta_{ij} \quad (11)$$

Where μ_t is the subgrid scale stress Smagorinsky-Lilly model for turbulent viscosity, which is defined by,

$$\mu_t=\rho\left[\min(kdC_sV^{1/3}\right]^2|\bar{S}|^2 \quad (12)$$

With *k*=0.42 (the von Karman constant), *d* is the distance to the closest wall, *Cs* is the Smagorinsky constant, and *V* is the volume of the computational cellule.

τ_{kk} is the normal components of the subgrid-scale stresses and $\bar{S}_{ij}$ is the rate-of-strain tensor for the resolved scale,

defined by:

$$\bar{S}_{ij} = \frac{1}{2}\left(\frac{\partial \bar{u}_i}{\partial x_j} + \frac{\partial \bar{u}_j}{\partial x_i}\right) \quad (13)$$

II.2.3 Velocity profile simulation

At fully developed flow regime, the velocity profile rearrangement over the flow passage section has a uniform profile, either in the laminar where the profile has a parabolic form or in the turbulent regime where the profile is flat. Several profile velocity expressions can be found in the literature, which describes the velocity distribution, among other we can cite; a uniform velocity profile, a power law velocity, and a parabolic velocity profile. The velocity profiles calculation is well-founded on the branches dimensions and the incoming nominal flow for each test carried out during the simulation. The velocity distribution across a cylindrical tube in our case can be approximated using the well-known power law relationship velocity profile [12] where:

$$u(r) = u_{max}\left(1 - \frac{r}{R}\right)^{\frac{1}{n}} \quad (14)$$

u_{max} is the maximum velocity at the pipe centerline (m/s). R is the pipe radius, r is the varying radius (m), which take a value from 0 to R. n is a constant coefficient depending on the Reynolds Number. The ratio between the average velocity and the velocity centerline of the tube is given by:

$$\frac{u}{u_{max}} = \frac{2n^2}{(n+1)(2n+1)} \quad (15)$$

with $n = \frac{1}{\sqrt{f}}$, and f is the friction coefficient.

II.3. Initial and Boundary conditions

The calculations are performed on a parallel configuration with eight processors (CPUs) running at a frequency of 2.66 GHz each and with a RAM memory of 16 GB. The simulated physical phenomenon has a duration of 12 seconds, with a time step Δt = 0.05 s. For this test, we are using the reference flow rates from the Vattenfall experimental setup, which serve as the basis for our simulation. The respective flow rates for the cold pipe and hot pipe are 9 l/s with an inlet temperature of 19 °C, and 6 l/s with an inlet temperature of 36 °C.

The axial velocity injection for cold main pipe and secondary hot pipe have initially a variable distribution. Since the thermal mixing takes place in the mixing area (Fig. 1), and because the simulation with LES takes a long time, it is not advantageous to model the whole configuration. For this, just a part of the main pipe length will be taken into consideration in the calculation.

In the initial phase of this study, a mesh sensitivity analysis was conducted to determine the impact of mesh variations on the simulation results. However, for the sake of simplicity in this written presentation, the results of this sensitivity analysis are not included in this document. To discretize the space domain for LES calculations, the SIMPLEC algorithm was chosen for pressure-velocity boundary condition, and a Second-order linear upwind scheme was adopted to approximate the convective fluxes for momentum and energy transport equations. A turbulent intensity of 5% was considered for all profiles. Nevertheless, a relatively fine grid of 2.3 million nodes (see Fig. 3) was meshed with hexahedral non-structured mesh. Near the wall, a refinement of the pipe was made to solve the small-scale turbulent motions. For this last reason, the standard Smagorinsky model [26] was used to model the turbulent viscosity for small scale eddies.

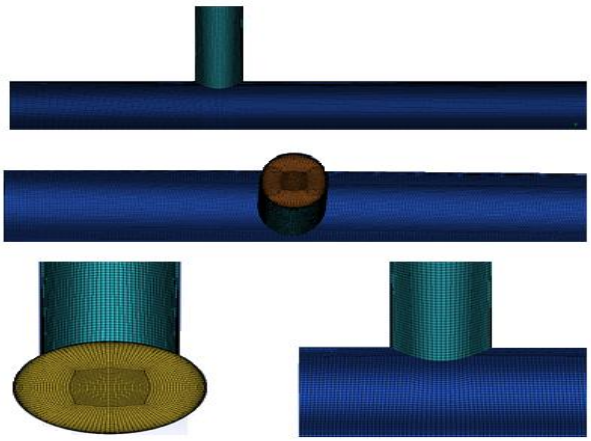

Figure 3. Computational domain meshes.

The temperatures of cold and hot working fluids are set at 19 °C and 36 °C, respectively (Fig. 4). The corresponding flow rates used in the benchmark tests are about 9 l/s for cold pipe, and 6 l/s for hot pipe. These values correspond to a ratio of 0.4 between the hot and cold pipe, while the Reynolds number are 7.9×10^4 and 1.07×10^5, respectively. All boundary conditions and the using data inputs necessary to the present simulation are summarized in Table 1.

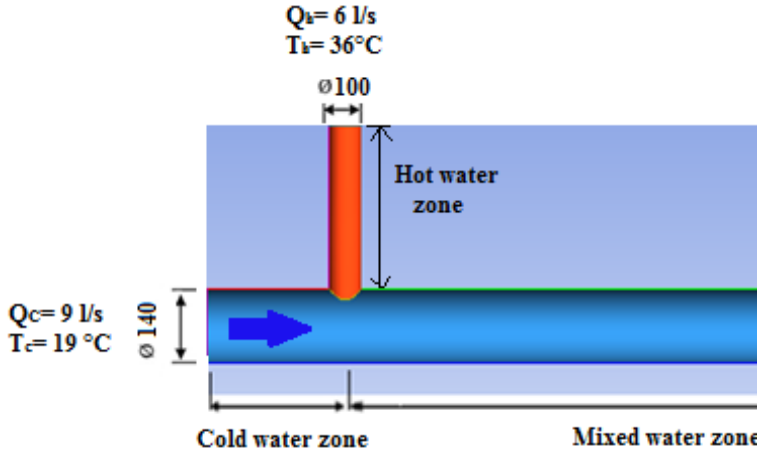

Figure 4. Computational domain for CFD simulations.

Table 1. Inlet input data for simulation [27].

Parameter	Temperature (°C)	Pipe diameter (mm)	Flow rate (l/s)
Vertical hot cold water pipe (D1)	36	100	6.0
Horizontal main cold water pipe (D2)	19	140	9.0

III. Results and discussions

This section presents a study using numerical simulation through CFD codes to analyze the temperature and flow velocity distribution in a T-junction using a power law velocity profile. The authors emphasized the valuable

contribution of numerical simulation through CFD in studying temperature mixing and optimizing the design of fluid mixing at different temperatures. This approach allows for a deeper understanding of thermal and fluid transfer phenomena in such configurations, offering perspectives for improvement and optimization of fluid mixing system performance in these geometric setups.

In summary, the simulation where performed between two numerical CFD models (SST and LES) and the results were compared with experimental data to validate their accuracy. The studied parameters included the geometry of the T-junction, inlet temperatures of the fluids, and fluid flow rates. The ANSYS CFX v19 code was used to solve the Navier-Stokes equations as well as the temperature transport equation for the two incoming fluid flows.

For simplicity, the presentation of the results utilizes dimensionless normalized temperature and velocity. This normalization allows for generalizing the CFD calculations and normalizing the results, focusing on relative thermal and dynamic behaviors and velocity distribution patterns. By normalizing temperatures and velocities using appropriate reference quantities, it becomes possible to compare results between different configuration cases. This facilitates trend analysis and generalization of conclusions. Moreover, the use of dimensionless temperature in Eq. (16) describes the actual temperature minus the cold flow inlet temperature, divided by the difference between hot and cold inlet temperatures [28]. The obtained results can be more easily extrapolated to other scales or operating conditions.

$$T^* = \frac{T_{actual} - T_c}{T_h - T_c} \quad (16)$$

The velocity profile was also normalized with a bulk velocity, in (m/s), which represent the average flow velocity for fluid flow in a pipe, defined as:

$$u_{bulk} = Q/(\pi r_c^2) \quad (17)$$

Where Q is the mean flow rate equal to 15 l/s.

III.1. Dynamic field

The results of spatial distribution of the average velocities in the mixing zone are presented in Figures 5 and 6, illustrating two different planes (vertical and horizontal) over a period of 12 seconds and for various locations. The measurements have been performed at four locations downstream of the T-junction (1.6D, 2.6D, 3.6D, 4.6D). This choice is to justify the fully developed flow can be obtained inside the pipe.

After calculation, an important observation was reported is that the velocity profile obtained by the LES simulation are in very good agreement with the experimental data, compared to those obtained by the SST turbulence model. This observation is consistent, as the LES model resolves the large-scale turbulence while modeling the effects of small scales, allowing feasible calculations at high Reynolds numbers. The simulation by LES model gives a better prediction of the velocity profiles to the experimental data for 4.6D test case in the center of the pipe at axial and vertical directions, where similar characteristics to an undisturbed free flow was observed. These profiles are more difficult to capture, because they are strongly influenced by the mixing zone and complicated to capture the flow characteristics in the region close to the T-junction connection [28]. However, on the pipe wall region, the experimental results were poorly predicted. Indeed, for all cases, a boundary layers were developed and the flow is slowed because the high momentum ratio (ratio of velocity of cold fluid to velocity at mixed fluid at outlet) of the branch pipe, consequently in this region, the velocity magnitude decrease until it will be lost [29]. In case of SST model simulation results, it can be observed that the curve deviates slightly from the experimental data, and the results are substantially higher than the measured value. This as result of the presence of higher turbulent intensity and this could be an indication that the averaging time assigned for SST simulation of about T~12s real time was still too short to get a reliable result. For this, it would be necessary to make a more refinement mesh to obtain more precise approximation, and devoted a longer time for simulation.

After the mixing area, the fluid is fully developed and reaches the hydraulic equilibrium; a state where the velocity profiles of a system can reach the turbulence velocity profiles. At hydraulic equilibrium condition, in our case the centerline velocity take a value of 1.1 m/s (Fig. 6), where is theoretically about 0.974 m/s [29]. The intensity of fluctuation and the corresponding thermal stress in the main and branch pipes are strongly influenced by the momentum ratio of the flows, which creates higher thermal load at the top of the pipe [30].

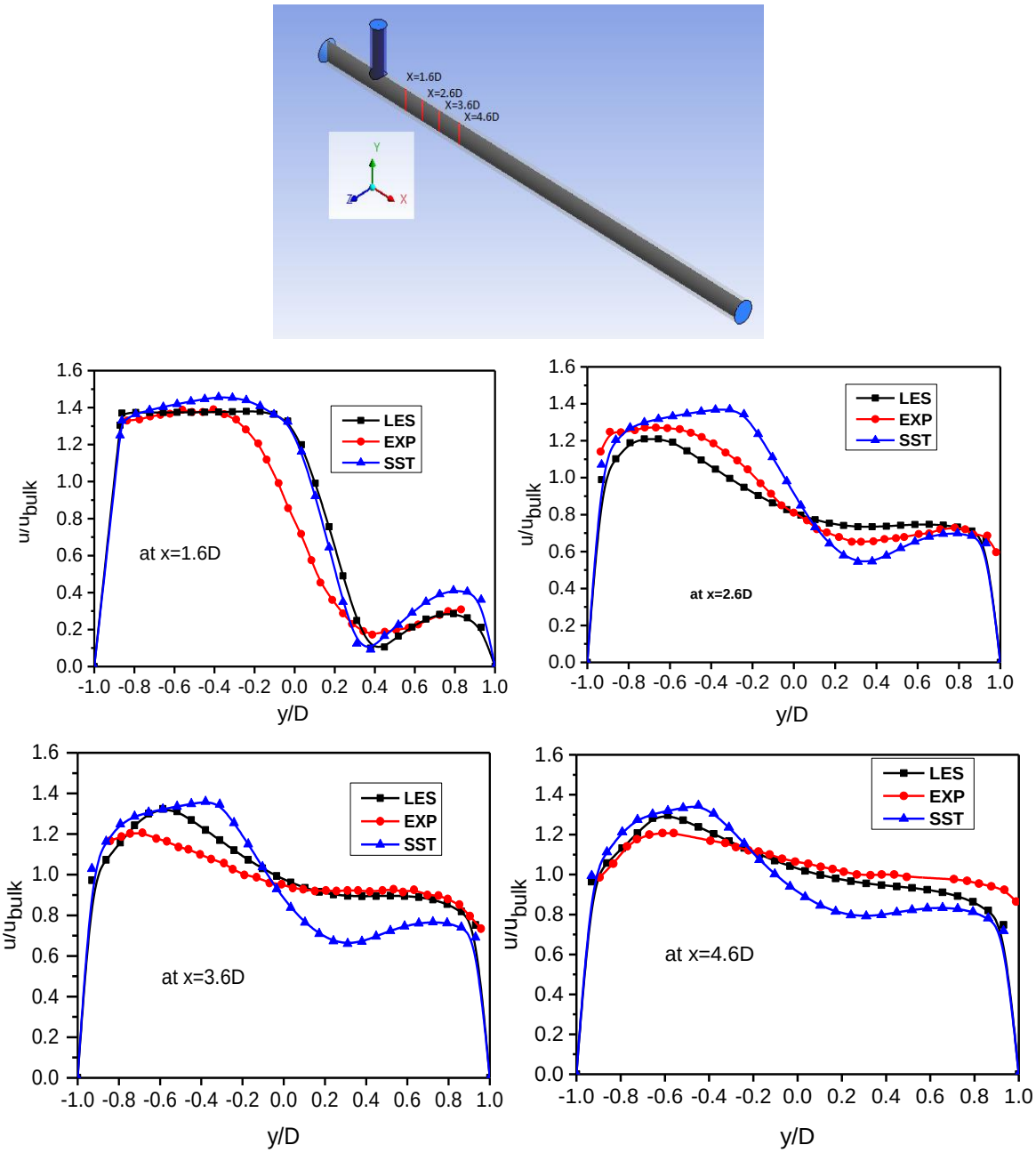

Figure 5. Time averaged velocity distributions for different locations at vertical direction.

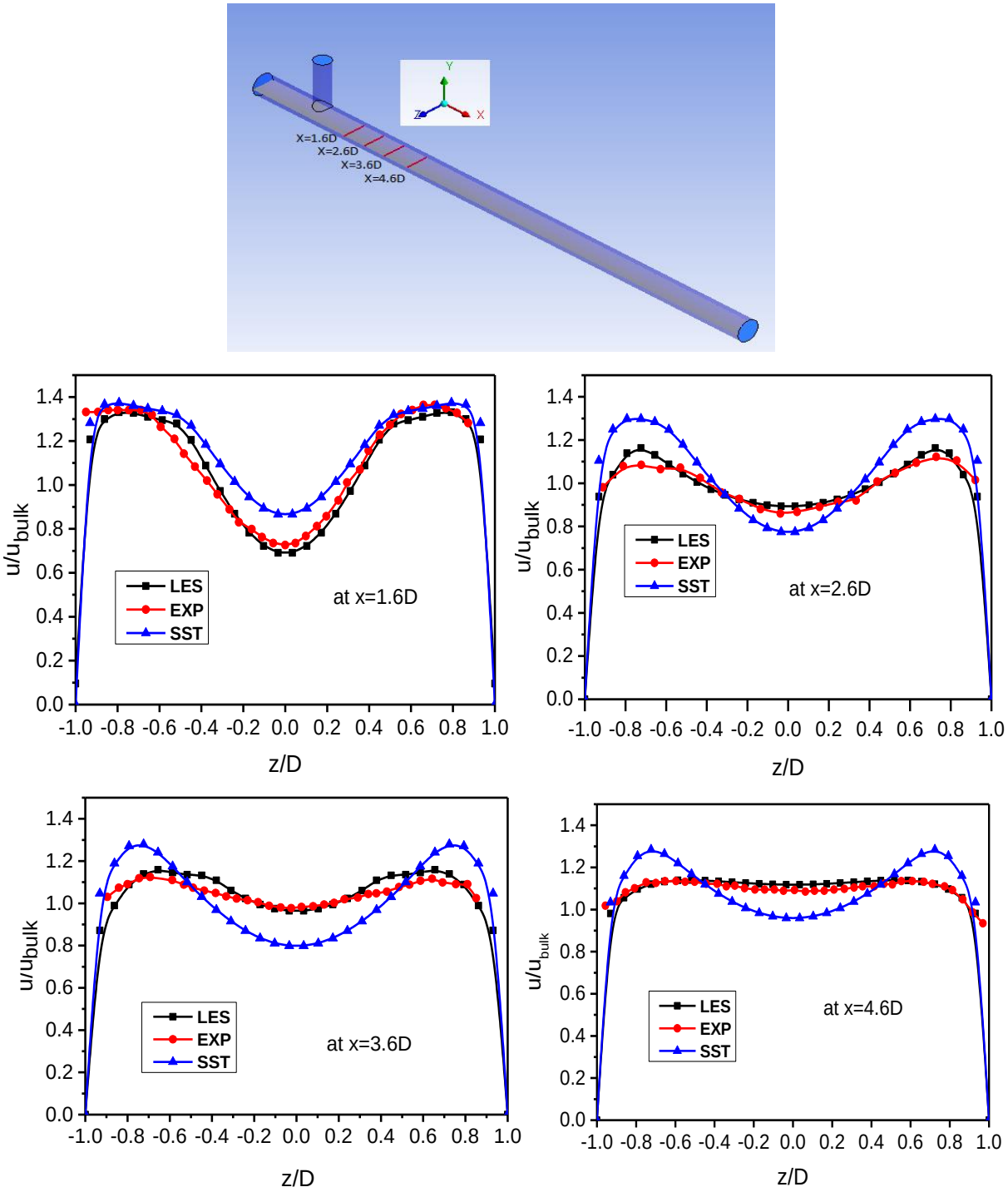

Figure 6. Time averaged velocity distributions for different locations at horizontal direction.

Figure 7 presents a detailed graphical image of the velocity field distribution in the mixing zone, both in the vertical and horizontal planes. The colors and contours in the image illustrate the velocity variations in different regions of the studied space, providing a clear and informative visualization. Furthermore, this figure highlights the recirculation zones, which correspond to the areas where the fluid flows in a cyclical or swirling manner. These recirculation zones are crucial for understanding the phenomenon of fluid mixing and circulation within the system. Then, when the hot and cold flows from the main and secondary pipes meet, shear instabilities produce turbulent vortices [31]. The recirculation zone in the upper part of the pipe near the T-junction is apparent, a phenomenon which will delay the mixing of the two fluids. However, the mean distribution cannot clearly describe the turbulence instabilities. From the preliminary results of Figure 7, it can be clearly seen that the use of the SST model gives quite good approximations in the analysis of turbulence characteristics and consequently in the evaluation of the fluctuations of the velocities and the temperature, while the LES gives some better turbulence

characteristics, where the eddies of mixing are produced due to shear layer instabilities [28]. The magnitude of the velocity gradient is sufficiently high in the mixing region. A high velocity gradient leads to an increase in the length needed to reach hydraulic and thermal equilibrium [10].

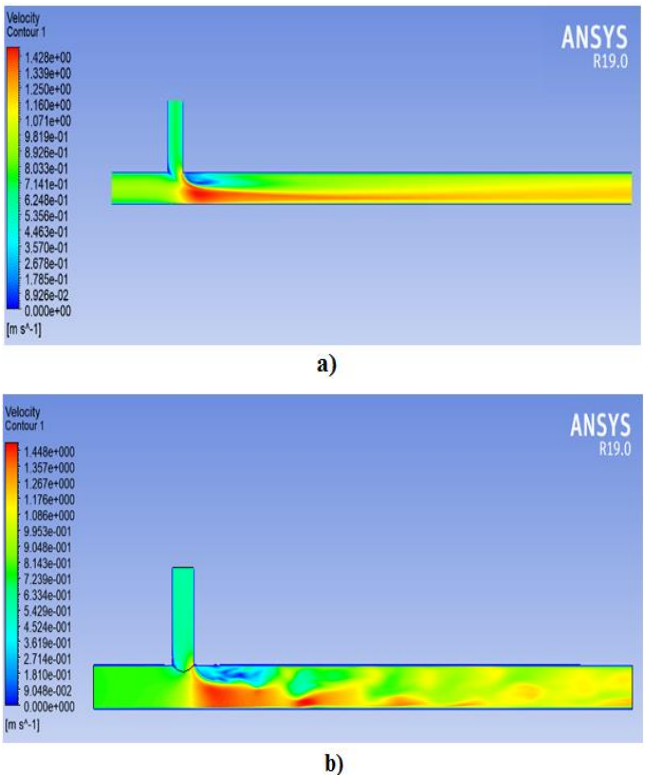

Figure 7. Time average velocity distribution at t=12s with; a) SST model, and b) LES model.

III.2. Temperature fluctuations

To predict the instantaneous temperature distribution in the cross section of the pipe, a vertical cut planes have been designed. It can be seen that the mixing phenomenon takes place for a relatively long distance further downstream of the T-junction. The extend mixing flow has led to develop and the propagation of high temperature gradient of liquid along the upper part of the main pipe [32] near the wall and the cold water the lower part. Figure 8 and 9 show the spatial temperature distribution using both CFD models. The separation of the two fluids is due to the effect of density and gravity. The density gradient is a consequence of the temperature difference which has a significant influence on the distribution of the mixture. A homogeneous flow at the end of the pipe covers almost the entire area of this section, which results in a thermal equilibrium where the two fluids reach the same average temperature.

Just at the exit of the brunch junction, where rapid collisions take place between the hot and cold fluids, the temperature difference take a maximum. At short distance from the mixing zone, the two fluids are not completely mixed, but after several diameters downstream of the T-junction the two fluids merge together (Figs. 8 and 9). However, the temperature gradient on the lowest part of the main pipe becomes more and more significant over time. The LES temperature values are more compatibles with the experimental data, where the SST model fail to predict a realistic mixing between the fluids, because this model tends to apply the statistical average data, which was not reached in the calculation. Furthermore, it was remarked that an inner recirculation zone was generated and developed at right corner of the T-brunch connection, which instantaneously decreases with turbulent dissipation along the tube. The presence of recirculation zone and instabilities in the flow promotes temperature diffusion and fluid mixing, leading to a more homogeneous distribution of temperatures along the main pipe.

Figure 10(a) shows the time-averaged temperature distribution contour in cross-sections defined with SST, while Figure 10(b) gives an overview about the high degree of mixing generated by the instabilities eddies occurs

not far from the center of the T-junction, where the temperature ranges from 295.6 °*K* to 308.7 °*K*.

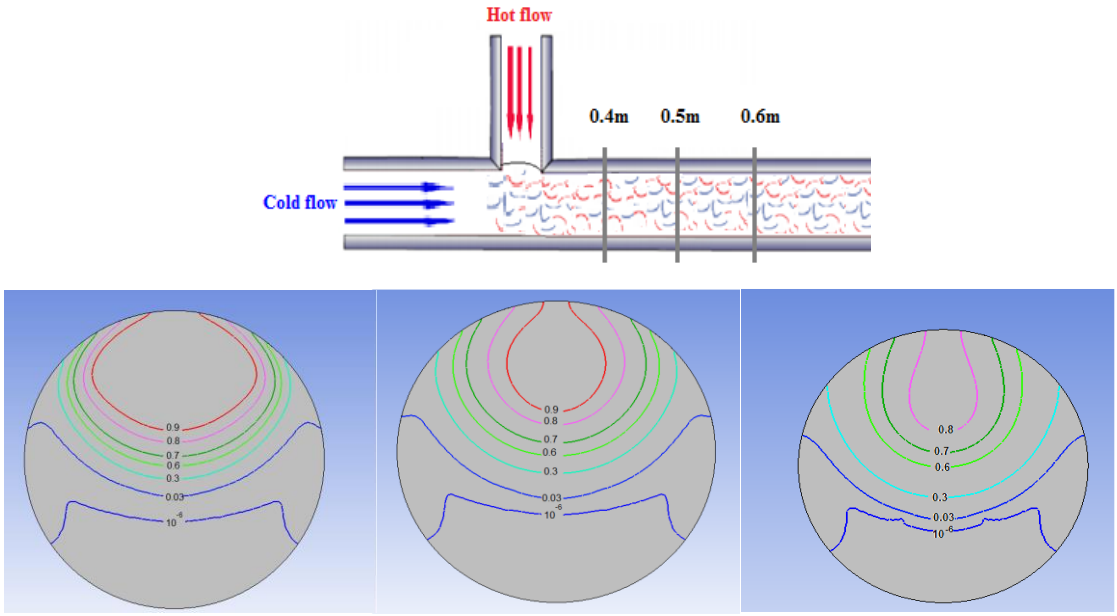

Figure 8. Spatial temperature distribution on transversal section on the main pipe using SST model.

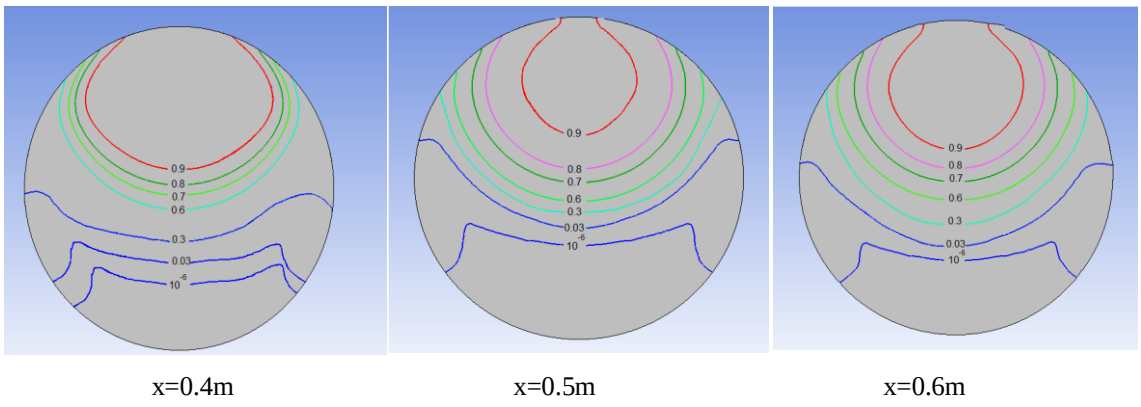

Fig. 9. Spatial temperature distribution on transversal section on the main pipe using LES model.

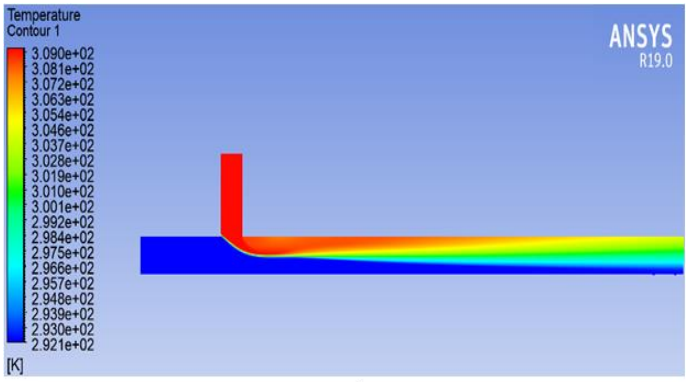

a)

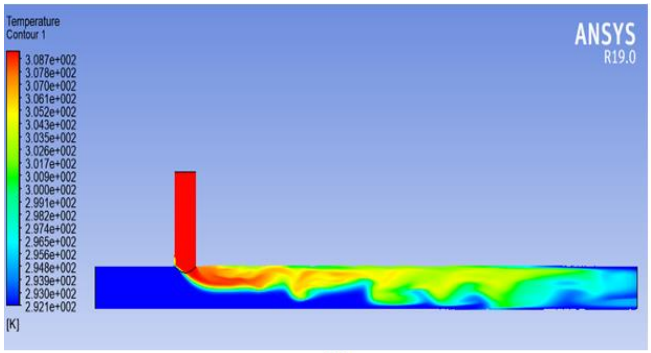

b)

Figure 10. Contour of temperature distribution at t=12s with; a) SST model, and b) LES model.

III.3. Normalized temperature

The analysis of the behaviour of mixed scalar T* is essential for understanding the thermal mixing processes and heat exchanges in the T-junction system. Temporal variations in thermal mixing can have a significant impact on the performance and efficiency of the system. The thermal mixing performance represent the degree of temperature mixing, which was rescaled by a nondimentional, also normalized temperature called mixing scalar, calculated by using Eq. (16). The temperature difference is the key factor to judge the quality of mixture; if the temperature difference is lower, the thermal mixing quality will be higher and mixing performance decreases with the increase of fluid temperature difference [33].

Figure 11 provides an analysis of spatio-temporal behavior of the mixed scalar T* downstream of mixing zone. The curves depict the distribution of thermal mixing at three different locations: top, middle, and bottom of the mixing zone, for this a vertical cut planes have been designed. The considered interval time is taken of 10 seconds. It can see that the thermal mixing performance is very low near the mixing zone, where the hot and cold fluid meet, and increases with the increase of distance. This observation is consistent with the turbulent mixing process occurring in the mixing zone.

The fully developed fluid reaches the thermal equilibrium; a state where the heat stops flowing and the two systems (hot and cold) reach the same mean time-averaged temperature. Both systems tend towards thermal equilibrium over time, a process that can take significantly longer time from one system to another. In our case, the mixing flow start to reach the thermal equilibrium after 4s simulation time (Fig. 11). After this, the magnitude of temperature at equilibrium continue to propagate along the tube in streamwise direction, and the change thereafter is insignificant. The maximum value of normalized temperature near the wall region at the top of the tube is about 0.65, where the scalar takes a values of 0.4 and 0.02, respectively in the medium position and the bottom of the tube. The difference between the last two values gives an indication about the magnitude of thermal load [29]. Close to the junction branch the thermal load is more significate than the region far from the mixing area.

The normalized temperature over simulation time of top, medium and bottom wall are shown in Figure 12. As presented in this figure, it can be observed that the normalized temperatures are well predicted with LES and have a good agreement with the experimental data especially at the top of the pipe. For the SST model the temperatures at the bottom of the pipe are underpredicted and at the top is overpredicted. This indicates that the thermal mixing predicted by SST need longer distance to be accomplished.

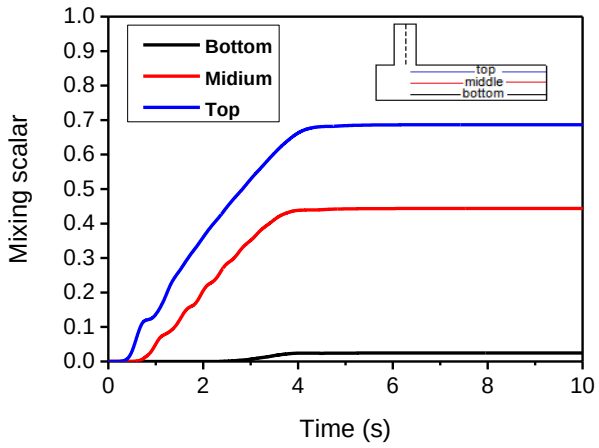

Figure 11. Temporal normalized temperature variation in the radial distance of the main pipe.

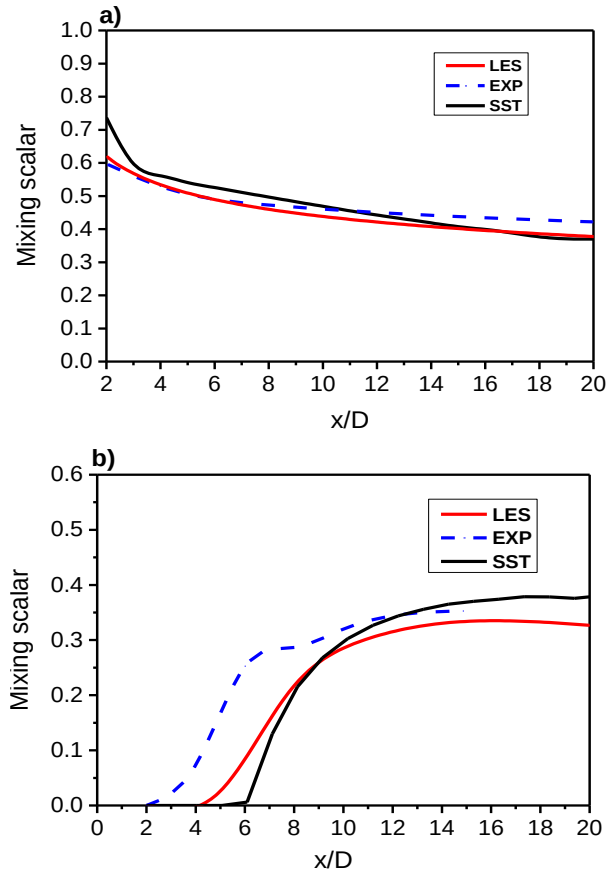

Figure 12. Spatial mixing scalar variation in the longitudinal direction of the main pipe;
a) at the top, b) at the bottom.

IV. Conclusion

In present work, the LES and the SST turbulence models have been used and compared to an experimental benchmark. The main objective is to predicting the mean flow field, the velocity and temperature of the turbulent mixing using a power law velocity profile. After calculation, we can conclude that the LES model considerably agrees well the experimental data for capturing the underlying physics of the turbulent thermal mixing phenomena in the T-junction, and they are more precise than SST model simulation. The intensity of fluctuation and thermal stress creates higher thermal load at the top of the pipe and reaches the hydraulic equilibrium first and the thermal

equilibrium. The magnitude of temperature at equilibrium, reach a maximum value of the normalized temperature at the top of the tube, where this scalar is less in the medium position and the bottom of the tube. After these results, we can conclude that close to the junction branch the thermal load is more significate than the region far from the mixing area. Furthermore, comparing the results with experimental data confirms the validity of the simulation models used and strengthens confidence in the drawn conclusions. This integrated approach between simulation and experimentation also opens new perspectives for optimizing thermal systems and developing more efficient and sustainable solutions.

Acknowledgements

This work was supported by funding from Nuclear Research Center of Birine/ Algerian Atomic Energy Commission (COMENA). The authors thank the Nuclear Research Center of Birine for all the help to get this work

References

[1] M. Boumaza, F. Moretti, R. Dizene, "Numerical simulation of flow and mixing in ROCOM facility using uniform and non-uniform inlet flow velocity profiles," Nucl. Eng. Des, Vol. 280, pp. 362–371, 2014. https://doi.org/10.1016/j.nucengdes.2014.10.018.

[2] N. Fukushima, K. Fukagata, N. Kasagi, H. Noguchi, K. Tanimoto, "Numerical and experimental study on turbulent thermal mixing in a T-junction flow," The 6th ASME-JSME Thermal Engineering Joint Conference, TED-AJ03-582, Big Island of Hawaii, Hawaii, March 16–20, 2003.

[3] B. L. Smith, J. H. Mahaffy, K.A. Angele, "A CFD benchmarking exercise based on flow mixing in a T-junction," Nuclear Engineering and Design, Vol. 264, pp.80–88, 2013. https://doi.org/10.1016/j.nucengdes. 2013.02.030.

[4] M. Weathered, J. Rei, M. Anderson, P. Brooks, "Coddington B. Characterization of thermal striping in liquid sodium with optical fiber sensors," Journal of Nuclear Radiation Sci, Vol. 3, No. 4, pp. 041003, 2017 (9 pages), https://doi.org/10.1115/1.4037118.

[5] M. Hirota, H. Asano, H. Nakayama, T. Asano, S. Hirayama, "Three-Dimensional Structure of Turbulent Flow in Mixing T-Junction," SME International Journal Series B, Vol. 49, No. 4, pp. 1070–1077, 2006. https://doi.org/10.1299/jsmeb.49.1070.

[6] C. Walker, M. Simiano, R. Zboray, H. M. Prasser, "Investigations on mixing phenomena in single-phase flow in a T-junction geometry," *Nuclear Engineering and Design*, Vol. 239, No. 1, pp. 116–126, 2009. https://doi.org/10.1016/j.nucengdes.2008.09.003.

[7] Z. Kun, H. Zhilong, Z. Sipeng, Y. Yingyuan, W. Wenhui, D. Kangyao, "Study on a new pressure loss model of T-junction for compressible flow with particle image velocimetry test," Proc. Inst. Mech. Eng. Part A, J. Power Energy, 2021. https://doi.org/10.1177/09576509211037638.

[8] Z. Wei-yu, L. Tao, J. Peixue, G. Zhi-jun, W. Kui-sheng, "Large eddy simulation of hot and cold fluids mixing in a T-junction for predicting thermal fluctuations," Applied Mathematics and Mechanics, Vol. 30, No. 11, pp. 1379–1392, 2009. https://doi.org/10.1007/s10483-009-1104-7.

[9] J. P. Simoneau, J. Champigny, O. Gelineau, "Applications of large eddy simulations in nuclear field, " Nucl. Eng. Des, Vol. 240, No. 2, pp. 429–439, 2010. https://doi.org/10.1016/j.nucengdes.2008.08.018.

[10] A. Frédéric, A. Toutant, R. Monod, G. Brillant, F. Bataille, " Numerical simulations of sodium mixing in a T-junction, " Applied Thermal Engineering, Vol. 37, pp. 38–43, 2012. https://doi.org/10.1016/j.applthermaleng. 2011.12.044

[11] R. Monod, "Étude des fluctuations de température par Simulations des Grandes Échelles," Doctorat thesis, (Energy and Environment), Perpignan Via Dominia University, 2012.

[12] J. Westin, P. Veber, L. Andersson, M. Carsten‘t, U. Andersson, J. Eriksson, J, M. E. Henriksson, F. Alavyoon, C. Andersson, "High-cycle thermal fatigue in mixing Tees: Large-Eddy simulations compared to a new validation experiment, " In: 16th Int. Conf. On Nuclear Engineering (ICONE-16-48731), pp. 1–11, 11–15 May 2009, Florida, Orlando, USA, https://doi.org/10.1115/ICO NE16-48731.

[13] Z. Mi, W. Fabian, K. Rudi, L. Eckart, "Large Eddy Simulation on thermal-mixing experiment at horizontal T-junction with varied flow temperature," Nuclear Engineering and Design, Vol. 388, pp. 111644, 2022. https://doi.org/10.1016/j. nucengdes.2021.111644.

[14] M. Kimura, H. Ogawa, N. Igarashi, H. Kamide, "Experimental study on fluid mixing phenomena in T-pipe junction with upstream elbow", Nuclear Engineering and Design, Vol. 240, pp. 3055–3066, 2010. https://doi.org/10. 016/j.nucengdes.2010.05.019.

[15] T. Lu, S. M. Liu, D. Attinger, "Large-eddy simulations of structure effects of an upstream elbow main pipe on hot and cold fluids mixing in a vertical tee junction", Annals of Nuclear Energy, Vol. 60, pp. 420–431, 2013. https://doi.org/10.1016/j.anucene. 2013.04.010.

[16] A. Yacine, lk. L. Jeong, "LES and URANS predictions of thermal load in piping systems: T-Junction," Proceedings of ICONE20 20th International Conference on Nuclear Engineering (ICONE20-54981), Anaheim, California, USA, July 30- August 03, 2012.

[17] T. Lu, W. Han, H. Zhai, "Numerical simulation of temperature fluctuation reduction by a vortex breaker in an elbow pipe with thermal stratification,"Annals of Nuclear Energy, Vol. 75, pp. 462–467, 2015. http://dx.doi.org/ 10.1016/j.anucene.2014. 08.067.

[18] V. S. Naik-Nimbalkar, A. W. Patwardhan, L. Banerjee, G. Padmakumar, G. Vaidyanathan, "Thermal mixing in T-junctions, " Chem. Eng. Sci, Vol. 65, No. 22, pp. 5901–5911, 2010. https://doi.org/10.1016/j. ces.2010.08.017.

[19] M. Kuschewski, R. Kulecovic, E. Laurien, "Experimental setup for the investigation of fluid structure interactions in a T-junction," Nuclear Engineering and Design, Vol. 264, pp. 223–230, 2013. https://doi.org/10.1016/j. nucengdes.2013.02.024.

[20] C. H. Lin, M. S. Chen, Y. M. Ferng, "Investigating thermal mixing and reverse flow characteristics in a T-junction by way of experiments, "Applied Thermal Engineering, Vol. 99, pp. 1171–1182, 2016. https://doi.org/10.1016/j.applthermaleng.2016.02.009.

[21] J. Westin, F. Alavyoon, L. Andersson, P. Veber, M. Henriksson, C. Andersson, "Experiments and Unsteady CFD-Calculations of Thermal Mixing in a T-Junction," OECD/NEA/IAEA In Proc. Workshop on the Benchmarking of CFD Codes for Application to Nuclear Reactor Safety (CFD4NRS), Munich- Germany, pp. 1–15, 2006.

[22] S. B. Pope, "Turbulent flows," Cambridge University press, Sussex, U. K, ISBN: 9780521598866, 2002. https://doi.org/10.1017/CBO9780511840531.

[23] F. R. Menter, "Two-equation eddy-viscosity turbulence models for engineering applications", AIAA Journal, Vol. 32, No. 8, pp.1598–1605, 1994.

[24] D. C. Wilcox, "Turbulence Modeling for CFD," Anaheim: DCW Industries, 3rd Edition, 2006, ISBN: 978-1-928729-08-2.

[25] D. C. Wilcox, "Re-assessment of the scale-determining equation for advanced turbulence models," AIAA Journal, Vol. 26, No. 11, pp. 1299–1310, 1998. https://doi.org/10.2514/3.10041.

[26] J. Smagorinsky, "General circulation experiments with the primitive equations," Mon. Wather Rev Vol. 91, pp. 99–164, 1963. https://doi.org/10.1175/1520-0493(1963)091<0099:GCEWTP>2.3.CO;2.

[27] Ansys Inc., "ANSYS Fluent user’s guide, " Release 15.0, pp. 695–758, November 2013.

[28] H. Thomas, "Scale resolved simulations of the OECD/NEA-Vattenfall T-junction benchmark," Nuclear Engineering and Design, 2014. https://doi.org/10.1016/j. nucengdes.2013.08.021.

[29] A. Hüseyin, N. S. Cemal, "CFD modeling of thermal mixing in a T-junction geometry using LES model," Nuclear Engineering and Design, Vol. 253, pp.183–191, 2012. https://doi.org/10.1016/j.nucengdes.2012. 08.010.

[30] B. Debashis, H. Mohammed, D. Kaushik, "Turbulence induced thermal mixing effects and thermal fatigue analysis in T-junction configurations in pressurized water reactors (PWR)," Proceedings of the 2nd Thermal and Fluid Engineering Conference, TFEC2017, 4th International Workshop on Heat Transfer, IWHT2017, Las Vegas, NV, USA, April 2–5, 2017.

[31] K. Sun-Hye, C. Jae-Boong, P. Jung-Soon, C. Young-Hwan, L. and Jin-Ho, "A coupled CFD-FEM analysis on the Safety Injection Piping subject to thermal lamination," Nuclear Engineering &. Technics, Vol. 45, No. 2, 2012. http://dx.do.org/10.5516/net.09.2012.038.

[32] B. Ulrich, E. Paolo, "Numerical analysis of two experiments related to thermal fatigue," Nuclear Engineering and Technology, Vol. 49, pp. 675–691, 2017. https://doi.org/10.1016/j.net.2017.01.018.

[33] C. Mei-Shiue, H. Huai-En, F. Yuh-Ming, P. Bau-Shi, "Experimental observations of thermal mixing characteristics in T-junction piping," Nuclear Engineering & Design, Vol. 276, pp. 107-114, 2014. https://doi.org/10.1016/j. nucengdes.2014.03.052.